

Evaluation of Seismic Performance of Reinforced Concrete Buildings by Damage Spectrum Method

K. Tajima & N. Shirai

Nihon University, Tokyo, Japan

A. Nishio

Shimizu Corporation, Tokyo, Japan

K. Imai

KozoSoft Co.,LTD, Tokyo, Japan



SUMMARY:

Damage spectra were constructed using recorded ground motions during the Eastern Japan Earthquake in 2011. Such parameters as design spectra, strength reduction factor and force-displacement relationship characterizing damage spectrum were established with reference to the seismic code in Japan and past research works. Other parameters were calibrated through comparison of damage indices derived from damage spectra and observed damage states of the affected R/C buildings. Furthermore, over-strength factor was introduced to consider difference between expected design strength and actual strength of buildings. As a result, damage indices derived from the damage spectrum were in good agreement with damage level of the affected R/C buildings.

Keywords: R/C building, Damage Spectrum, Eastern Japan Earthquake Disaster, Over-strength, Aftershock

1. INTRODUCTION

Through lessons from the “Eastern Japan Earthquake Disaster” occurred in March 11, 2011, several issues can be raised regarding the damage evaluation of existing reinforced concrete (R/C) buildings. First, the current damage evaluation procedure was not able to identify an area of heavily affected buildings immediately after earthquake. Unfortunately, serious accident of the nuclear power plants occurred along with the disaster over a wide area. For this reason, it was difficult to collect inclusive damage information of buildings rapidly. AIJ (Architectural Institute of Japan) began with the damage investigation of buildings over all affected areas in the Eastern Japan, and results were reported in April 6, 2011. Second issue is twofold: there were several buildings with no damage among the buildings judged to be seismically insufficient by the Standard of Seismic Assessment of Existing R/C Buildings in Japan (2001), and on the contrary some of seismically retrofitted buildings were suffered from damages. According to the seismic assessment method, seismic capacity shall be evaluated on the basis of energy calculated as product of strength and ductility of building under an equivalent static lateral force. If the seismic capacity is judged to be insufficient, retrofitting of the building must be required to improve its capacity. Unfortunately, the seismic assessment method does not take an interactive effect of fundamental period of ground motions and buildings into consideration. However, actual capacity of the building may be changed depending on type of input ground motions and site conditions. Final issue is effect of aftershock. Very strong aftershock occurred at Sendai city in April 7, 2011 after the main shock on the day before. In fact, these damages were recognized by the investigation of school buildings in Sendai city. In order to evaluate actual residual capacity of the building against aftershock as well as main shock, first damages by the main shock shall be evaluated, and then the damage evaluation against maximum probable aftershock must be required. However, damages for all events including aftershocks cannot be simply accumulated, because dominant direction and period of ground motions may be changed, and fundamental period of buildings may become longer due to the damage accumulation.

Concept of damage spectrum proposed by Bertero et al. (2004) is useful to cope with these issues. The damage spectrum is defined as variation of damage index, DI, against natural period for a series of SDOF systems subjected to recorded ground accelerations. Thus, this index can include effect of

shaking characteristics of ground motion and site conditions on the damage evaluation. If the damage spectrum for ground motion recorded at arbitrary locations or expected earthquakes can be constructed, damage level of building against earthquake can be predicted in terms of natural period of the building. In the present study, special attention is paid to the damage evaluation of buildings by means of the damage spectrum, and effort is made to extend this method to refined damage evaluation method. In this study, validity of the damage spectrum by Bertero et al. is investigated through comparison with observed actual damages of the affected buildings during the Eastern Japan Earthquake Disaster, and a refined damage evaluation method is presented by solving difficulties encountered in the current method. Validity of the refined damage spectrum is demonstrated by comparing the damage spectra constructed using recorded ground motions of main shock and aftershocks by the strong motion network, K-NET and KiK-net, of the National Research Institute of Earth Science and Disaster Prevention with observed actual damage states of buildings located near by the recording stations.

2. DAMAGE SPECTRUM

The damage spectrum represents variation of damage index, DI , against natural period, T (sec), for a series of SDOF systems. The damage index will be $DI = 0$ if the structure remains elastic (no damage), and will be $DI = 1.0$ if structural collapse is expected. Other states correspond to DI values between 0 and 1.0. Bozorgnia and Bertero(2001) improved the damage index, DI_{PA} , for R/C components proposed by Park et al.(1985), and introduced two new damage indices, DI_1 and DI_2 , for inelastic SDOF systems. They are expressed as a combination of maximum deformation and hysteretic energy dissipation capacity. Aim of this improvement was to remove the following defects on DI_{PA} :

- First, for elastic response, DI_{PA} value will be greater than 0.
- Next, if the maximum deformation capacity is reached under monotonic deformation, DI_{PA} value will be greater than 1.0.

Formulae for the damage indices, DI_{PA} , DI_1 and DI_2 , have been defined as follows:

$$DI_{PA} = (u_{\max}/u_{\text{mon}}) + \beta(E_H/E_{H\text{mon}}) \quad (2.1)$$

$$DI_1 = \{(1 - \alpha_1)(\mu - \mu_e/\mu_{\text{mon}} - 1)\} + \alpha_1(E_H/E_{H\text{mon}}) \quad (2.2)$$

$$DI_2 = \{(1 - \alpha_2)(\mu - \mu_e/\mu_{\text{mon}} - 1)\} + \alpha_2(E_H/E_{H\text{mon}})^{1/2} \quad (2.3)$$

where u_{\max} = maximum deformation, u_{mon} = maximum deformation capacity under monotonic deformation, E_H = hysteretic energy dissipation, $E_{H\text{mon}}$ = hysteretic energy capacity under monotonic deformation, $\mu = u_{\max}/u_y$ = displacement ductility, u_y = yield deformation, μ_e = ratio of maximum elastic deformation to yield deformation, $\mu_{\text{mon}} = u_{\text{mon}}/u_y$ = monotonic ductility capacity, β = constant, and α_1, α_2 = coefficients. Note that E_H in Eq.(2.3) can be converted to an equivalent hysteretic velocity by the following relationship (Akiyama, 1985):

$$V_H = \sqrt{2E_H/M} \quad (2.4)$$

where V_H = Equivalent velocity of hysteretic energy, and M = mass. DI_{PA} in Eq.(2.1) proposed by Park et al. has been calibrated against numerous experimental and field observations. It is also known that DI_{PA} corresponds to the damage category in Table 2.1. Thus, the indices, DI_1 and DI_2 , shall be consistent with this damage category.

For constructing the damage spectrum, it must be required to specify several parameters as shown in Fig.2.1. They includes: (1) elastic design spectrum, (2) strength reduction factor R_d , and (3) monotonic ductility capacity μ_{mon} . For example, Bertero et al. specified these parameters as (1) UBC-97, (2) $R_d = 3.4$, and (3) $\mu_{\text{mon}} = 8$ or 10. However, these parameters may not be always applicable to buildings in Japan, because Japanese code may be different from UBC-97. In addition, although Bertero et al. have used elastic-perfectly-plastic (EPP) model as force-deformation relationship, it may not be representative of R/C structures. Furthermore, since application of the damage category listed in Table 2.1 is prerequisite for calibrating α_1 and α_2 in Eqs.(2.2) and (2.3), the coefficients, α_1 and α_2 , should be

determined so that DI_1 and DI_2 would be consistent with DI_{PA} . Bertero et al. determined coefficients, α_1 and α_2 , by comparing values of DI_1 and DI_2 with those of DI_{PA} for $0.2 < DI_{PA} < 0.8$. For instance, using 220 horizontal ground acceleration records of the Northridge earthquake in 1994 and 176 horizontal ground acceleration records of Lander earthquake in 1992, the coefficients were estimated through regression analysis to be $\alpha_1=0.27$ and $\alpha_2=0.30$ for $\mu_{mon}=10$.

Table 2.1. Categorization of Damage

Damage	Physical Appearance	DI_{PA}
COLLAPSE	Total or Partial Collapse of Building.	1.0~
SEVERE	Extensive Crashing of Concrete. Disclosure of Buckled Reinforcements.	0.4~1.0
MODERATE	Extensive Large Cracks. Spalling of Concrete in Weaker Elements.	0.25~0.4
MINOR	Minor Cracks Throughout Building. Partial Crashing of Concrete in Columns.	0.1~0.25
SLIGHT	Sporadic Occurrence of Cracking	0~0.1

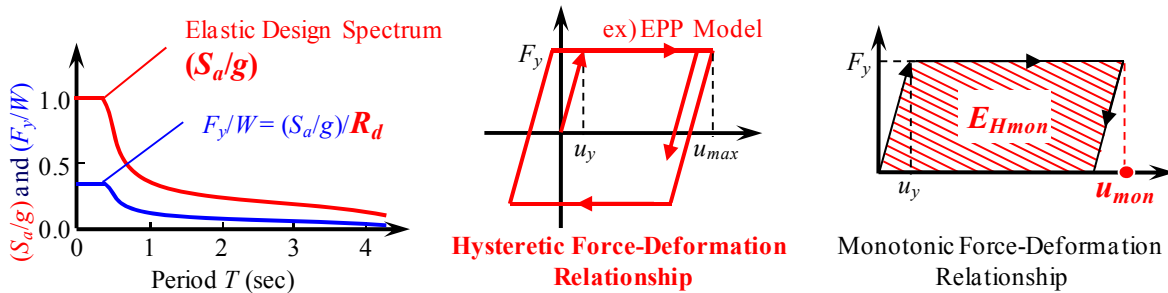


Figure 2.1. Parameters for Damage Spectra

3. ASSUMPTION OF PARAMETERS FOR DAMAGE SPECTRUM

3.1. Design Spectrum

As indicated in Fig.2.1, SDOF system is assumed to have 5% viscous damping and force-displacement relationship with yield strength F_y based on the elastic design spectrum reduced by factor, R_d . First of all, it must determine the yield strength, F_y . However, specified design spectrum in Japan has been changed with revision of the seismic design code in 1981, and thus expected strength of building may vary depending on seismic design procedure to be applied. In this study, distinction between code before 1981(referred to as “old seismic code”) and one after 1981(referred to as “new seismic code”) is made. For buildings designed according to the new seismic code, the design response acceleration spectrum shown in Fig.3.1(a) is applied. On the other hand, the old seismic code specified lateral seismic intensity of 0.2 under moderate level of ground motions, and buildings were designed against equivalent static lateral forces according to the allowable stress design procedure. In other words, since design spectrum can not be specified, it is rather difficult to estimate yield strength, F_y . For this reason, a correction factor, λ , with respect to an equivalent force of $0.2W$ corresponding to the seismic intensity of 0.2, as shown in Fig.3.1(b), shall be introduced.

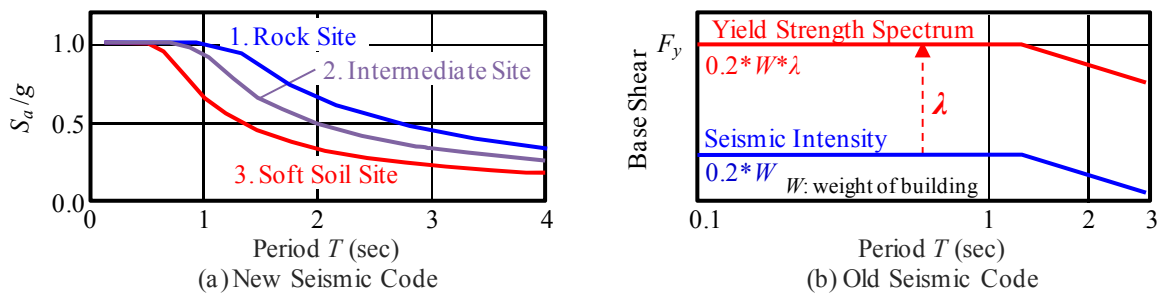


Figure 3.1. Design Spectrum and Yield Strength of Japanese Earthquake-Resistant Standard

For estimating value of the correction factor λ , four R/C buildings listed in Table 3.1 were selected to be investigated. Buildings A and B were affected R/C school buildings and damage investigation at the sites was done by the authors. Framed structures were modelled with reference to the drawings and specifications, and yield strength, F_y , was calculated by the pushover analysis. Figure 3.2 shows framing elevation of Building A. Although there are quite a few beams and columns with adjacent non-structural walls, beams and columns including non-structural walls were modelled by fibre elements. Slabs were assumed to be rigid diaphragms and modelled by truss elements. As is seen in Fig.3.3, the columns with adjacent non-structural walls tend to become shear-critical short columns. To simulate shear behaviour in such columns, shear sub-element was incorporated into the column. Note that this shear sub-element is able to simulate softening behaviour after shear failure (Tajima et al, 2010). Stress-strain relationships for concrete (Concrete01) and steel (Steel01) are shown in Fig.3.4. Numerical analyses were carried out using an open source code called ‘‘OpenSees’’. Also, the confined model on core concrete proposed by Mander (1988) was included. Stiffness after steel yielding was assumed to be one percent of Young’s modulus, E_s . After gravity loads were imposed on tops of columns at each level, the pushover analysis was executed under load control based on an assumed A_i pattern of lateral forces. On the other hand, as far as two full-scale existing buildings are concerned, yield strengths were determined from their respective test results. Consequently, average value for λ was roughly estimated to be 4.3.

3.2. Seismic Design Strength Reduction Factor

Ishiyama et al. (2006) evaluated earthquake damage in R/C buildings by means of DI_{PA} and effect of the cumulative damage was introduced into strength reduction factor, R_D . This factor depends on soil conditions and is defined as follows:

$$R_D = \frac{\mu_{mon} - 1}{\Phi} + 1 \quad (3.1)$$

$$\Phi = 1 + \frac{1}{\left(2.75 - \mu_u^{0.28}\right) T^{0.6}} - \frac{1}{1.8T} \exp\left[-0.6(\ln T - 0.5)^2\right] \quad (\text{Rock Site}) \quad (3.2)$$

$$\Phi = 1.3 + \frac{1}{\left(4 - \mu_u^{0.45}\right) T^{0.75}} - \frac{1}{1.65T} \exp\left[-3.4(\ln T + 0.1)^2\right] \quad (\text{Intermediate Site}) \quad (3.3)$$

$$\Phi = 1.3 + \frac{1}{3\mu_u^{-0.5} \left(\frac{T}{T_g}\right)} - \frac{1}{1.2 \left(\frac{T}{T_g}\right)} \exp\left[-6 \left(\ln \frac{T}{T_g} - 0.16\right)^2\right] \quad (\text{Soft Soil Site}) \quad (3.4)$$

where T = natural period and T_g = predominant period of ground motion. R_D -factor by Ishiyama shall be used in this study, and prior to its application, site conditions at the measuring stations of K-NET and KiK-net must be categorized. Accordingly, the categorization of IBC2009 (2009) adopted is listed in Table 3.2. Note that IBC2009 is based on average velocity of soil shear waves (AVS30) propagating in soil layers down to depth of 30m.

3.3. Hysteretic Force-Deformation Relationship

Bertero et al. used EPP model as force-deformation relationship to construct the damage spectrum, but EPP model may not be representative of R/C structures. Instead, Clough model, which is one of the most popular models for R/C structures as shown in Fig.3.5, shall be applied in this study. In order to simulate deterioration with increase in the ductility factor, unloading stiffness, K_r , of Clough model was determined as follows:

$$K_r = \mu_i^{-\gamma} K_0 \quad (3.5)$$

where μ_i = ductility factor, γ = degradation factor of unloading stiffness(=0.5), and K_0 = initial stiffness.

Table 3.1. λ for Buildings Designed According to Old Earthquake-Resistant Standard in Japan

	Weight W (kN)	$0.2W$ (kN)	Yield Strength F_y (kN)	λ
School Building A	19,695	3939	15,800	4.0
School Building B	39,393	7879	25,000	3.2
Existing RC School Building (Yokouchi et al, 2004)	4,076	815	2,906	3.6
Full-Scale 3-Story RC Building (Kabeyasawa et al, 2008)	3,536	707	4,597	6.5

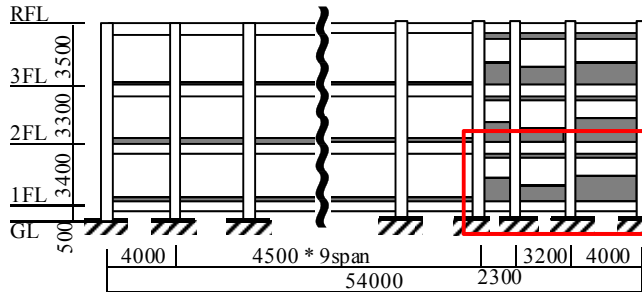


Figure 3.2. Flaming Elevation of Building A

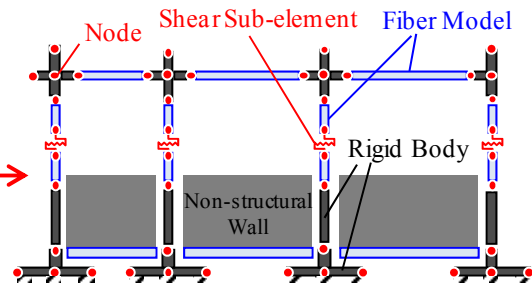


Figure 3.3. Modeling of Column with Shear Sub-element

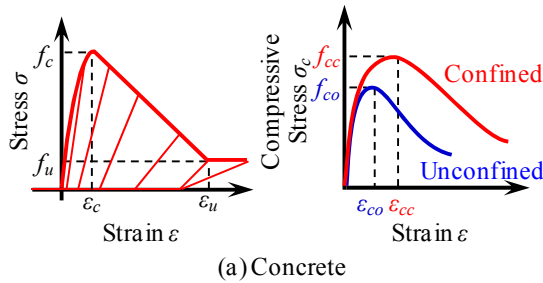


Figure 3.4. Stress-Strain Relationships of Concrete and Steel

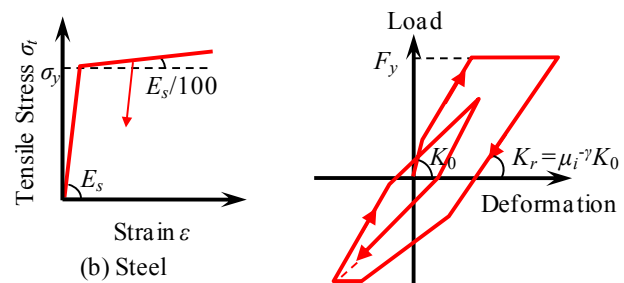


Figure 3.5. Clough Model

Table 3.2. Categorization of Site Condition

Site Class	IBC2009		Ishiyama et. al
	Soil Profile Name	Soil Shear Wave Velocity V_s (cm/s)	Soil Profile Name
A	Hard Rock	$1524 < V_s$	Rock Site
B	Rock	$762 < V_s < 1524$	
C	Very Dense Soil and Soft Rock	$366 < V_s < 762$	Intermediate Site
D	Stiff Soil Profile	$183 < V_s < 366$	
E	Soft Soil Profile	$V_s < 183$	Soft Soil Site

3.4. Monotonic Displacement Ductility Capacity

In recent years, several full-scale specimens of R/C buildings have been tested under alternate cyclic loading. However, little data on the ductility capacity μ_{mon} of R/C buildings under monotonically increasing lateral deformation is available, although μ_{mon} is a key parameter influencing on the damage spectrum. For this reason, rough estimate on μ_{mon} shall be done by comparing calculated value of the damage index with observed damage level in buildings nearby measuring station of ground motions.

3.4.1. List of Damaged Buildings

Damaged buildings to be investigated are listed in Table 3.3. Figure 3.6 shows pictures of affected buildings, being representative of each damage category. Information listed in Table 3.6 was prepared with reference to the reconnaissance reports of AIJ (2011) and BRI (2011) as well as the damage investigation by authors. The damage level corresponds to one indicated in Table 2.1. Natural period of the buildings was estimated either from micro-tremor measurements or an approximate formula; $T=0.015H$; H is building height in meter. As a rule, value indicated in the design drawings and specifications shall be used for H . But if not available, height of each story was identically assumed to

be 3.9 m. This value is average story height of the buildings listed in Table 3.3.

Table 3.3. List of Damaged Buildings

	Standard	Natural Period T (sec)	Degree of Damage
A	Old	0.16*	SLIGHT
B		0.18*	SLIGHT
C		0.18*	SLIGHT
D ²⁾		0.23	SEVERE
E ²⁾		0.23	COLLAPSE
F ¹⁾		0.12	COLLAPSE
G ²⁾		0.82	MODERATE
H ¹⁾		0.23	MODERATE
I	New	0.25*	NONE
J ²⁾		0.29	MODERATE
K		0.33	MODERATE
L		0.23	MINOR
M		0.24*	SLIGHT
N		0.29*	NONE

1) AIJ, 2) Building Research Institute

*Micro-tremor Measurement



C : SLIGHT L : MINOR H : MODERATE



D : SEVERE E : COLLAPSE

Figure 3.6. Picture of Damaged Buildings

3.4.2. Identification of β -Value in Equation of DI_{PA}

Coefficients, α_1 and α_2 , shall be calibrated so that DI_1 and DI_2 would be consistent with DI_{PA} . Thus, it is possible to identify μ_{mon} directly from the damage index DI_{PA} without calibration of α_1 and α_2 . Note that a range of DI_{PA} must be $0.2 < DI_{PA} < 0.8$ in this identification. Parameters of β and u_{mon} are required to calculate value of DI_{PA} from Eq.(2.1). Since $\mu_{mon} = u_{mon}/u_y$, μ_{mon} shall be investigated instead of u_{mon} in the following subsection. Here, a way to identify the parameter, β , shall be investigated. Park et al. presented a formula for estimating β -value of a single R/C component as:

$$\beta = \left(-0.447 + 0.73 \frac{l}{d} + 0.24n_0 + 0.314p_t \right) \times 0.7^{\rho_w} \quad (3.6)$$

where l/d = shear span ratio, n_0 = normalized axial stress, p_t = longitudinal steel ratio as a percentage, and ρ_w = confinement ratio. However, to extend β defined in Eq.(3.6) to one for overall building, β -values calculated for all components must be averaged or integrated in a some way. This leads to rather complicated procedure. For simplicity, an effort shall be made to find a way for calculating an approximate value of β . First of all, the most influential parameter on β among four parameters in Eq.(3.6) is extracted. For this purpose, database consisting of 87 R/C column specimens tested in Japan was constructed. Then, correlation between values of four parameters and β -value for each column was examined. As is seen in Fig.3.7, there is good correlation between longitudinal steel ratio p_t and β , independent of their failure modes. Authors conducted the damage investigation on R/C school buildings after the Eastern Japan Earthquake. Fortunately, the detailed drawings and specifications were available from 21 buildings in 10 schools; 19 buildings by the old code and 2 buildings by the new code. It was found that an average value of longitudinal steel ratios for all columns in 21 buildings was 1.2 percent. Consequently, an approximate value of β was obtained to be 0.2 with reference to Fig.3.7.

3.4.3. Identification of Approximate Value for μ_{mon}

An approximate value of μ_{mon} shall be identified for affected buildings designed according to the old seismic code, using values of DI_{PA} ranging from 0.2 to 0.8. Here, Building G; moderate damage and $0.25 < DI_{PA} < 0.4$, and Building D; severe damage and $0.4 < DI_{PA} < 1.0$, listed in Table 3.3 were selected for identification of μ_{mon} . Figure 3.8 shows the damage spectra, DI_{PA} , for buildings G and D constructed using ground motions recorded by nearby the stations. The ordinate indicates DI_{PA} and its values are plotted against values of μ_{mon} with some deviation. It seems that value of 12 and 6 is suitable for μ_{mon} of Buildings G and D. Reason of discrepancy in μ_{mon} -values for the buildings of G and

D may be related to their failure modes. In Building G, although many cracks were observed in non-structural walls along the total height of building, severe shear crack was not observed in beams and columns. Thus, the failure mode of Building G may be judged to be flexural failure type. On the other hand, as is seen in Fig.3.6, severe shear failures in short columns were observed. From the discussion in the above, the value of μ_{mon} shall be 12 for flexure-critical building, and 6 for shear-critical building.

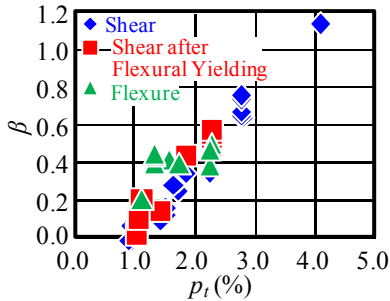


Figure 3.7. $\beta-p_t$ Relation

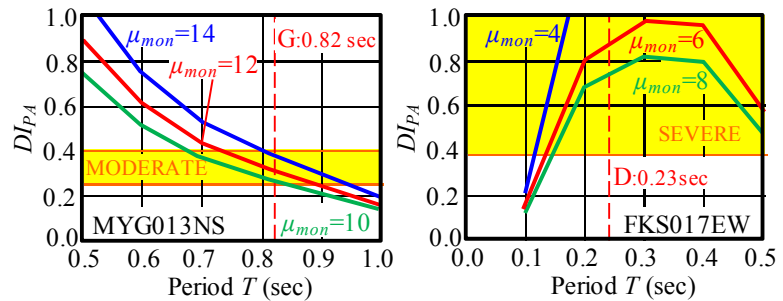


Figure 3.8. Damage Spectrum by DI_{PA}

3.5. Calibration of Approximate Value for α_1 and α_2

Values for β and μ_{mon} were identified in the previous section. In this section, α_1 and α_2 , which are coefficients in the formulae for DI_1 and DI_2 , shall be calibrated using the identified values of β and μ_{mon} . Damage spectra on the basis of DI_{PA} were constructed using twelve ground motions recorded at different stations during the Eastern Japan Earthquake in 2011. Then, the coefficients of α_1 and α_2 were determined against periods within a range of $0.2 < DI_{PA} < 0.8$. Figure 3.9 shows relationship between α_1 or α_2 and period T . α_1 -values show some scatters, especially significant in case of $\mu_{mon} = 6$. On the other hand, α_2 -values show almost identical tendency, irrespective of differences in ground motions and periods. From the above discussion, α_2 was assumed to be 0.4 for $\mu_{mon} = 6$ and 0.3 for $\mu_{mon}=12$, and DI_2 shall be used for the damage index in this study.

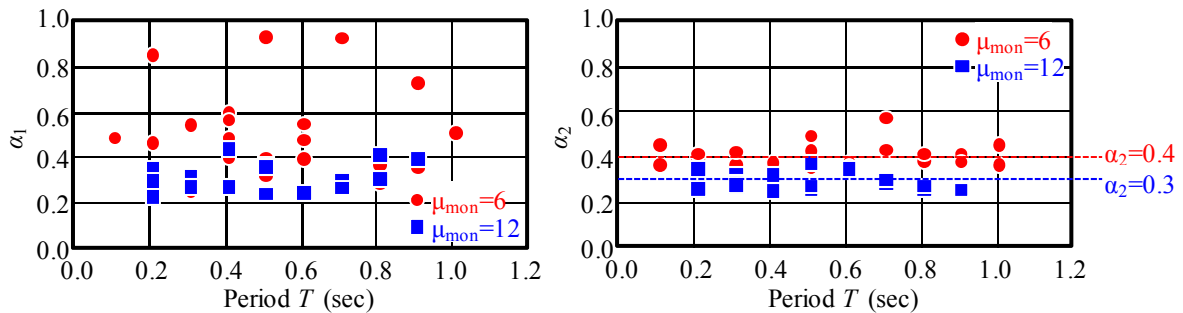


Figure 3.9. $\alpha_1, \alpha_2 - T$ Relation

4. VERIFICATION OF DAMAGE SPECTRUM WITH IMPROVED PARAMETERS

4.1. Damage Evaluation of Buildings Designed According to Old Seismic Code

Values of DI_2 are calculated for the buildings of A~H listed in Table 3.3 and they are compared with observed damage levels. Note that DI_2 -values for two directions; that is, E-W and N-S directions, are calculated independently. It must be noted that damage level in Table 3.3 includes effect of not only the main shock on March 11 but also aftershocks on damages. Thus, a series of acceleration records were generated by adding the acceleration records during the aftershocks to one of the main shock as shown in Fig.4.1. Value of μ_{mon} was assumed to be 6 for the buildings of D, E and F with the damage level of severe or collapse and 12 for other buildings. Figure 4.2 shows relation between DI_2 and

damage level. It can be confirmed that DI_2 with improved parameters reasonably corresponds to the observed damage level for all buildings.

4.2. Damage Evaluation of Buildings Designed According to New Seismic Code

Values of DI_2 are calculated for the buildings of I~N listed in Table 3.3 and they are compared with the observed damage levels. Yield strength, F_y , was specified on the basis of the design response spectrum of acceleration in Japan as shown in Fig.3.1. Value of μ_{mon} was assumed to be 12. Consequently, all calculated values of DI_2 were over 1.0, and thus they indicated overestimation of damage in comparison with the observed damage level. This may be due to effect of over-strength (Park, 1996). Over-strength is defined as difference between expected design strength, V_d , and actual strength, V_y , of buildings, and their ratio is referred to as the over-strength factor, Ω (see Fig.4.3). The over-strength stems from uncertainties such as difference between specified and actual strengths of material, contribution of non-structural components and confinement effect. Also, various safety factors to be considered in design may be related to the over-strength. In recent years, several values for the over-strength factor have been presented; for example, $\Omega = 1.67$ is recommended in Canada (CCBFC, 1995). Note that for buildings according to the old seismic code, correction factor, λ , shall be introduced to include additional contribution to actual strength as well as the over-strength factor. In this study, the over-strength factor, Ω , for the buildings of J~M were determined by a trial and error method. As a result, the factor, Ω , was determined to be 2.5 for J, 3.3 for K, 3.0 for L and 3.4 for M. Yield strength, F_y , was redefined by applying an average value of Ω 's to the buildings of I and N, and by applying respective Ω -value to other buildings. Now, Fig.4.2 indicates good correlation between estimated DI_2 -values and the observed damage levels.

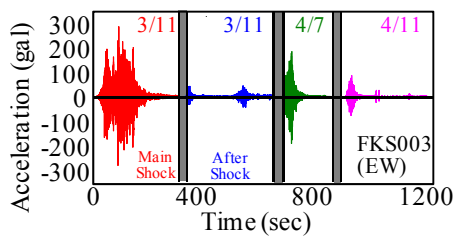


Figure 4.1. Composite Acceleration Record

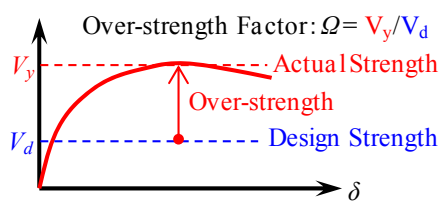


Figure 4.3. Over-strength Factor Ω

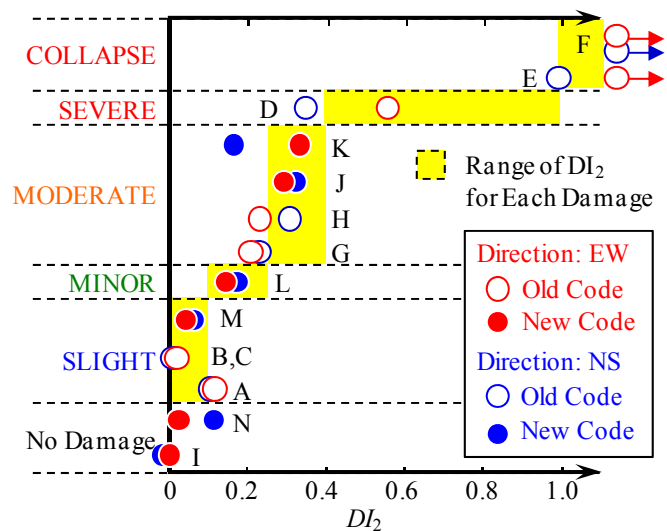


Figure 4.2. Damage Level- DI_2 Relation

4.3. Evaluation of Damages by Aftershock

Impact of aftershock on damage in R/C buildings shall be investigated using the recorded ground motions at Sendai-city shown in Fig.4.4.(a). Three set of ground motions were combined; first set includes main shock only (case-1), second set aftershock only (case-2) and third set main plus after shock (case-3). Figure 4.4.(b) shows damage spectra for Building K constructed with these ground motions. For case-1, DI_2 's were estimated to be 0.24(NS) and 0.08(EW). Thus, impact of NS motion on damage level is significant. For case-2, on the other hand, DI_2 's were estimated to be 0.12(NS) and 0.31(EW), and impact of EW motion on damage level is significant. This suggests that damage level induced may depend on intensity and direction of motions. For case-3, DI_2 's turned out to be 0.32(NS) and 0.36(EW), and thus the damage level was raised from those in case-1 and 2. It must be noted that the damage in NS direction changed from minor to moderate level, and is consistent with the observed damage state.

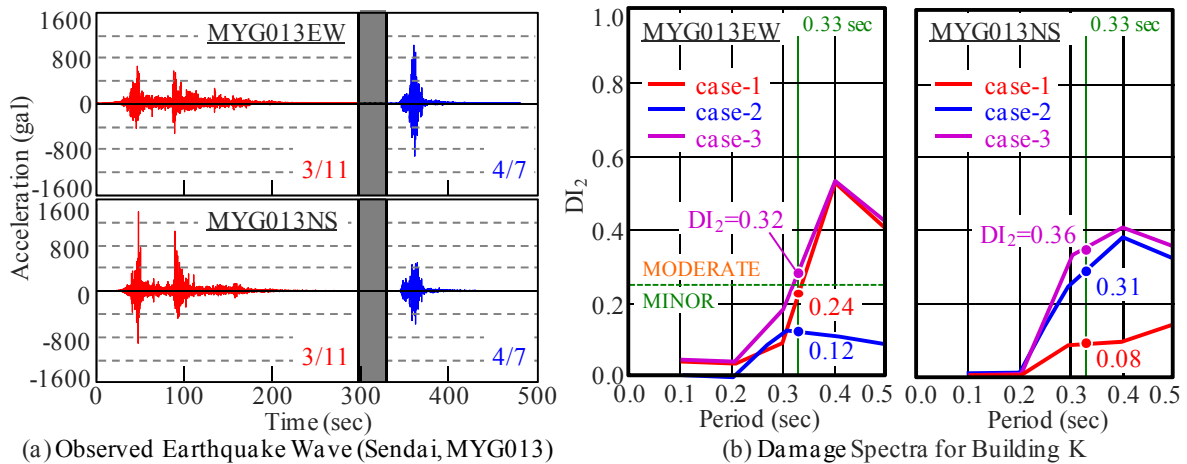


Figure 4.4. Impact of Aftershock on Damage

5. CONCLUSION AND FUTURE WORKS

Validity of the damage spectrum method has been investigated through the comparison of damage indices derived from the damage spectrum and observed damage states of the affected R/C buildings during the Eastern Japan Earthquake in 2011. The following findings were obtained:

- (1) To extend concept of the damage spectrum to the old or new seismic code in Japan, relationship between design response spectra of acceleration and yield strength was examined. For buildings designed according to the old seismic code, correction factor, λ , defined as ratio of actual strength to design strength, must be introduced, and an approximate value of 4.3 was identified for λ .
- (2) To construct the damage spectrum, the strength reduction factor R_d was introduced along with inclusion of site conditions and cumulative damages. In addition, Clough model, which is representative of behavior for R/C buildings, was adopted as force-deformation relationship.
- (3) Ductility factor capacity, μ_{mon} , under monotonic lateral deformation was investigated. As a result, an approximate value of μ_{mon} was determined to be 12 for flexure-critical buildings and 6 for shear-critical buildings. Furthermore, coefficients, α_1 and α_2 , were calibrated, and calibrated values for α_2 indicate roughly a constant value with small deviation independent of variation of ground motions and periods. Consequently, an approximate value of α_2 was determined to be 0.3 or 0.4 for flexure- or shear-critical buildings.
- (4) In case of buildings by the old code, the damage index, DI_2 , could be corresponded to the observed damage states by introduction of the correction factor, λ and μ_{mon} , depending on failure mode. In case of buildings by the new code, the damage index, DI_2 , could be corresponded to the observed damage states by introduction of the over-strength factor, Ω . Although further study is needed, it is recommended to use 3.0 for Ω within a range of current study.
- (5) Impact of the aftershock on damage accumulation in buildings was investigated using the recorded ground motions during main shock and aftershocks at Sendai-city. Damage evolution due to the aftershocks was verified by means of the damage spectrum.

Finally, a tentative integrated damage evaluation procedure is shown in Fig.5.1, although some of work is still remained for future investigation. First phase of damage evaluation is intended to grasp overall damage information of R/C buildings over affected areas by earthquake ground motions, and this will be quickly accomplished by utilizing the damage spectrum. The damage spectrum can also be applicable to development of the hazard map against expected earthquake ground motions. In this phase, R/C buildings will be screened using the damage index, and buildings with insufficient seismic capacity should be extracted. In second phase, extracted buildings shall be replaced with a MDOF lumped mass model or framed model. Then, earthquake response analysis on the model shall be carried out, and damage levels at each story as well as those of each component shall be estimated.

Through this process, defective parts in the building may be extracted, and parts or locations required for repairing and retrofitting can be specified. When such important buildings as public offices, schools and hospitals are to be investigated, proceeds to third phase. In this phase, expected explicit damages and their sources shall be clarified through simulation with advanced numerical tools like 3 dimensional finite element method, and safety of buildings shall be highly controlled and managed.

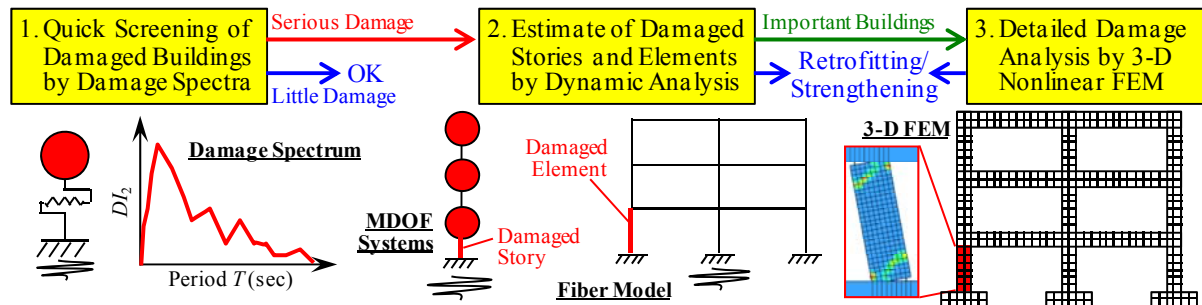


Figure 5.1. Proposed Damage Evaluation Procedure

ACKNOWLEDGEMENT

This research was partially supported by Japan Society for the Promotion of Science under Grant-in-Aid for Scientific Research (C) (Head Investigator: Prof. Shirai). The authors express their thanks to board of education, city office and principals at Sendai City, Fukushima City and Utsunomiya City for their contribution to the field survey. The strong motion records used in this study were provided by K-NET and KiK-net.

REFERENCES

- Akiyama, H. (1985). Earthquake-resistant limit-state design for buildings, University of Tokyo Press
- Architectural Institute of Japan. (2011). Preliminary Reconnaissance Report of 2011 Tohoku-Chiho Taiheiyo-Oki Earthquake, Architectural Institute of Japan
- Bozorgnia, Y. and Bertero, V.V. (2003). Damage Spectra: Characteristics and Applications to Seismic Risk Reduction, *Journal of Structural Engineering* **129:10**, 1330-1340
- Building Research Institute. (2001). Standard for Seismic Evaluation of Existing Reinforced Concrete Buildings, 2001, The Japan Building Disaster Prevention Association
- Building Research Institute (2011). Quick Report of the Field Survey and Research on “The 2011 off the Pacific coast of Tohoku Earthquake” (the Great East Japan Earthquake), *Building Research Data* **132**
- CCBFC (Canadian Commission on Building and Fire Code). (1995). National Building Code of Canada 1995, National Research Council of Canada, Ottawa, Ontario
- DE Guzman, P., Midorikawa, M., Asari, T. and Ishiyama Y. (2006) Evaluation of Seismic Design Strength Reduction Factor Considering Cumulative Damage and Site Conditions, *ournal of structural and construction engineering. Transactions of AIJ* **71:607**, 73-80
- Kabeyasawa, T., Kabeyasawa, T., Matsumori, T. Kabeyasawa, T. and Kim, Y. (2008). Shake Table Test on a Full-Scale Three-Story Reinforced Concrete Building Structure, *Journal of structural and construction engineering. Transactions of AIJ* **73:632**, 1833-1840 (in Japanese)
- Mander, J.B. (1988). Theoretical Stress-Strain Model for Confined Concrete, *journal of Structural Engineering* **114:8**, 1804-1826
- Park, Y.J. and Ang, A.H.S. (1985). Mechanistic Seismic Damage Model for Reinforced Concrete, *Journal of Structural Engineering* **111:4**, 722-739
- Park, Y.J., Ang, A.H.S. and Wen, Y.K. (1985). Seismic Damage Analysis of Reinforced Concrete Buildings, *Journal of Structural Engineering* **111:4**, 740-757
- Park, R. (1996). Explicit Incorporation of Element and Structure Overstrength in the Design Process, *In proceedings 11th World Conference on Earthquake Engineering*, Paper No. 2130
- Tajima, K., Shirai, N., Ozaki, E. and Imai, K. (2010). FE Modeling and Fiber Modeling for RC Column failing in Shear after Flexural Yielding, *Computational Modelling of Concrete Structures, Proceedings of Euro-C 2010*, 737-748
- Yokouchi, H., Kitajima, K., Ageta, H., Chikui, H., Nakanishi, M. and Adachi, H. (2004). Pseudo-Dynamic Test on an Existing R/C School Building Retrofitted with Friction Dampers, *13th World Conference on Earthquake Engineering*, Paper No. 2111